Single molecule measurements with photoelectron emission microscopy

Xianhua Kong, J. E. Rowe and R. J. Nemanich

Citation: Journal of Vacuum Science & Technology B: Microelectronics and Nanometer Structures Processing, Measurement, and Phenomena **26**, 1461 (2008); doi: 10.1116/1.2932094

View online: https://doi.org/10.1116/1.2932094

View Table of Contents: https://avs.scitation.org/toc/jvn/26/4

Published by the American Institute of Physics

ARTICLES YOU MAY BE INTERESTED IN

Doping profile of InP nanowires directly imaged by photoemission electron microscopy
Applied Physics Letters **99**, 233113 (2011); https://doi.org/10.1063/1.3662933

Single molecule measurements with photoelectron emission microscopy

Xianhua Kong and J. E. Rowe[a)]
Department of Physics, North Carolina State University, Raleigh, North Carolina 27695-8202

R. J. Nemanich
Department of Physics, Arizona State University, Tempe, Arizona 85287-1504

(Received 21 February 2008; accepted 28 April 2008; published 15 August 2008)

In this research, variable wavelength photoelectron emission microscopy (PEEM) with tunable UV light from the Duke University free electron laser is applied to image single fibrinogen molecules adsorbed onto *n*-type silicon surfaces. High resolution PEEM images (~10 nm) are obtained with photon energies from 4 to 6 eV. Wavelength-dependent image sequences are analyzed to determine the photoionization spectrum and the photoelectron emission threshold of individual molecules. The experimental data are fitted using temperature dependent Fowler law, square-root law, and cube-root law. The details of the theoretical models are discussed. The square-root and cube-root fittings reveal the ionization threshold of 5.0 eV for fibrinogen adsorbed onto *n*-type silicon, while temperature dependent Fowler law shows a threshold of 4.9 eV. The accuracy of the measurements is calculated to be ±0.2 eV. The authors conclude that no significant difference is observed from the three theoretical fitting approaches. © *2008 American Vacuum Society.* [DOI: 10.1116/1.2932094]

I. INTRODUCTION

Human plasma fibrinogen is a protein found in human blood, which plays a central role in the process of homeostasis and thrombosis, by participating in blood coagulation and facilitating adhesion and aggregation of platelets.[1] Fibrinogen is a 340 kDa dimeric molecule consisting of two sets of three-stranded coiled coils that connect the distal globular regions (D fragments) and meet at the abutting disulfide rings in the center of the molecule. The mainframe structure of fibrinogen is sigmoidal in shape.[2–4] The crystal structure of native chicken fibrinogen is displayed in Fig. 1(a).[5] Figure 1(b) presents the earlier model of fibrinogen.[6] It displays a trinodular structure (has three structural units), which consists of a central E and two outer D globular domains. The molecular length is 47.5 nm, with the roughly spherical D and E domains being 6.5 and 5 nm in diameter, respectively.

Human plasma fibrinogen is one of the most relevant proteins that absorb into biomaterial surfaces. In applications of blood based sensors, the biological components specifically react or interact with the analyte or biomolecule of interest, resulting in a detectable chemical or physical change. In this research, fibrinogen interacts with the oxidized silicon surfaces, which we suggest results in charge transfer. Nonspecific adsorption induced by fibrinogen molecules needs to be minimized for biocompatibility concerns. On the other hand, fibrinogen may be a factor for sensing homeostasis and thrombosis. The adsorption process may bring changes in conformation and function of proteins, depending on the particular properties of the surface in which the proteins are absorbed. These changes may promote subsequent reactions such as inflammation, activation of the immune system, or thrombosis.[7,8] Therefore, investigating the interactions between single molecules and surfaces is of interest.

The technique of photoelectron emission microscopy (PEEM), which involves imaging photoelectrons excited from the surface of a sample, is a powerful approach for obtaining spatially resolved images of biological samples. While images have been reported for viruses and DNA,[9] eukaryotic cells,[10] cultured cancer cells,[11] and cytoskeletons,[12] quantitative characteristics are difficult to obtain. Recently, we have exploited the tunability of the Duke OK-4 free electron laser (FEL) to determine the photothreshold of melanosomes isolated from human hair.[13] The square-root Fowler law was used in the fitting procedure to obtain the threshold. In this research, the photoionization threshold potential was determined for single molecules of human plasma fibrinogen adsorbed onto *n*-type Si. We discussed three theoretical models, including the temperature dependent Fowler law, square-root law, and cube-root law, to describe the photoemission process of a single biological molecule.

II. EXPERIMENTAL DETAILS

A. Fibrinogen adsorbed silicon surfaces

Plasminogen depleted human plasma fibrinogen, with a supplier specified purity of 95%, was purchased from Calbiochem in a lyophilized form. The process of lyophilization includes freeze drying and subsequent evaporation of the water in high vacuum; it is often used for tissue, blood, serum, or other biological substances. Then it was aliquoted in stocks and stored at −70 °C, which involves storing the solution in a number of smaller volume samples. The lyophilized protein was first placed on top of a phosphate buffer (10 mM K_2HPO_4/KH_2PO_4, 154 mM NaCl, and *p*H 7.4) in a water bath at 37 °C for 3 h at a concentration of 200 μg/mL. Then it was aliquoted in stocks and stored at −70 °C, which involves storing the solution in a number of smaller volume samples. Prior to use, the stock solution was thawed at 37 °C for 30 min and then diluted in the phos-

a)Electronic mail: rowe@unity.ncsu.edu

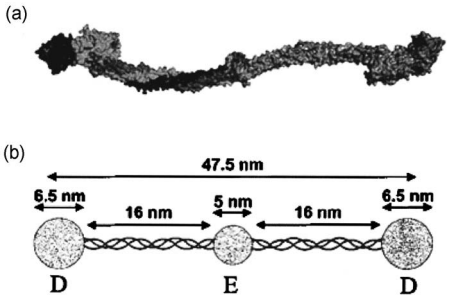

FIG. 1. Crystal structure of native chicken fibrinogen is shown in (a) with two sets of three-stranded coiled coils that connect the distal globular regions (D fragments) and meet at the abutting disulfide rings in the center of the molecule. The mainframe structure of fibrinogen is sigmoidal in shape (Ref. 5). A simplified model of fibrinogen is shown in (b) with a trinodular structure, which consists of a central E and two outer D globular domains (Ref. 6). The molecular length is 47.5 nm, with the roughly spherical D and E domains being 6.5 and 5 nm in diameter, respectively.

phate buffer to a final concentration of 1 μg/mL. A new solution was made each time before the deposition. The silicon substrate was *n*-type silicon (100) (resistivity of 0.05–0.1 Ω cm) obtained from Virginia Semiconductor, Inc. Before deposition of fibrinogen, the silicon wafer sections were cleaned using the RCA standard cleaning 1 process ($NH_4OH:H_2O_2:H_2O=0.25:1:5$, 80 °C, 10 min) to remove particles, followed by a 10 min UV ozone exposure to remove the hydrocarbon contamination. After dipping in 10% hydrofluoric acid to remove the oxidized layer, the Si samples were exposed to UV ozone again for 10 min to grow a well formed oxidized film with an approximate thickness of 1 nm. Each silicon substrate was immersed in a 25 μl fibrinogen solution for 10 min, then rinsed with 2 ml of deionized water and dried with a nitrogen gas flow.

B. FEL-PEEM measurements

PEEM is an ultrahigh vacuum electron microscopy technique based on the emission of electrons from a surface that is illuminated by an ultraviolet light source. A schematic of the PEEM, including the lens column and part of the objective chamber, is displayed in Fig. 2. Electrons emitted from the sample pass through a perforated anode, which is held at a negative high voltage of −20 kV (which forms part of an immersion lens system), and are imaged with a fluorescent screen. A microchannel plate between the fluorescent screen and electron optics intensifies the image, and a charge coupled device (CCD) camera records the data. The field of view of the instrument can be varied between 1.5 and 185 μm. We utilized the spontaneous emission mode of the Duke UV-FEL in the spectral range of 206.5–310.1 nm (6.0–4.0 eV), with an energy full width at half-maximum of ~0.1 eV. The Duke OK-4 ultraviolet free electron laser (UV-FEL) and PEEM have been described in more detail previously.[14]

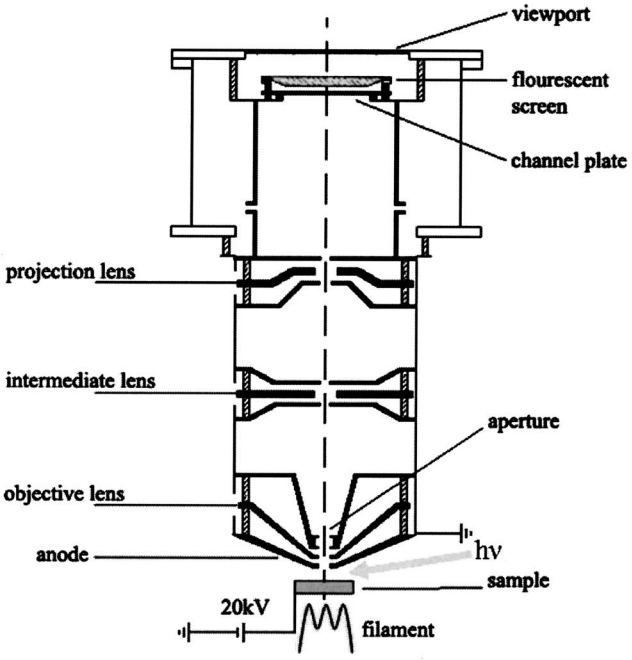

FIG. 2. Schematic of the PEEM used for our studies of fibrinogen adsorbed on Si surfaces. Electrons emitted from the sample pass through the anode (which is held at a negative high voltage of −20 kV and forms part of an immersion lens system). Additional magnification occurs with electrostatic and magnetic lenses with the magnified electrons, then amplified by a channel plate and imaged with a fluorescent screen.

C. Image processing

The PEEM images for each wavelength were acquired with a DVC 1312M digital camera from DVC Company, Inc. The camera resolution is 1300×1030 pixels×12 bits. The DVC VIEW program was used to display and save images. Single fibrinogen molecules were typically imaged at a field of view of 5 or 1.5 μm. The FEL spot size can be described as an elongated oval with axial dimensions of approximately 30 and 100 μm. The FEL focus was optimized for each wavelength.

One PEEM image for each wavelength of light, corresponding to a single data point on the photoionization threshold curves, was recorded using the above software and an area in each image, corresponding to one fibrinogen molecule, was then selected and saved as a separate image using the IMAGEJ software. The size and the shape of the selected region were kept constant between wavelength images using the image sequence option in the IMAGEJ software. At each image fragment, the intensity at each pixel was read and summed using MATLAB. This integrated brightness is taken to be proportional to the photocurrent collected from the region. Two additional data corrections were performed before analyzing the photoionization threshold. The software gain of the DVC imaging program was adjusted to avoid the black and white saturation. The integrated brightness was then corrected using the following equation:

$$\text{gain(dB)} = 20 \log_{10} G, \tag{1}$$

where G is the modification factor and "gain" is the gain level of the CCD camera in decibels (dB), which is read from

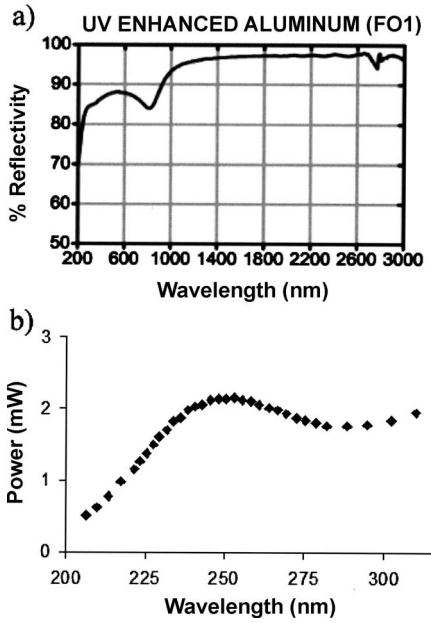

FIG. 3. UV enhanced aluminum (F01) mirror from Thorlabs is used to reflect the FEL beam in order to perform the power measurements. (a) shows their supplied reflectivity of the mirror over this wavelength range. The corrected power vs the wavelength of UV light is shown in (b), with the measurements taken at a distance corresponding to the position of the sample surface.

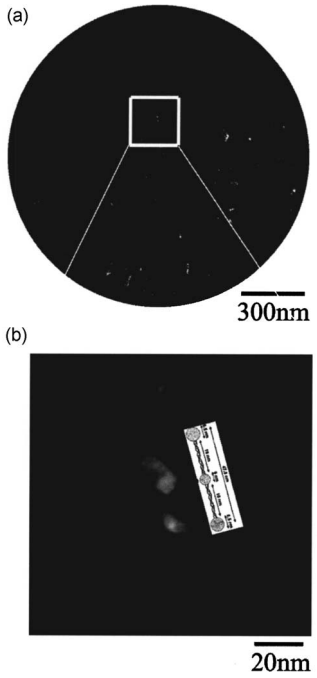

FIG. 4. PEEM image of fibrinogen adsorbed on *n*-type silicon that is illuminated by a spontaneous FEL emission at 238.5 nm (5.2 eV) is shown in (a) with a field of view of 1.5 μm. An enlarged section of the image is shown in (b) with the trinodular structure of fibrinogen. This inset in (b) displays the schematic of fibrinogen at a larger magnification, as indicated in the figure.

the DVC VIEW software. The incident photon flux at each wavelength of the FEL also affects the integrated brightness of the emitting region. The incident power of the spontaneous radiation at the sample surface in the PEEM depends on the current in the FEL storage ring and any absorption that may occur due to optics in the beam path. The upgrading of Duke OK-4 FEL to OK-5 in 2006 enabled maintaining a constant ring current of 100 ± 2 mA. In order to compensate the adsorption power, measurements for each wavelength were recorded at a distance similar to that for the sample in the microscope. An UV enhanced aluminum (F01) mirror from Thorlabs was used to reflect the FEL beam from the input port of the PEEM to the power meter. Figure 3(a) shows the mirror reflectivity at wavelength from 200 to 3000 nm adapted from the vendor. The power measurements were then corrected by using this data in Fig. 3(a). Figure 3(b) shows the incident power at each wavelength after corrections and the integrated brightness was normalized to a constant photon flux (photon per second).

III. RESULTS

A. FEL-PEEM imaging of single fibrinogen

Figure 4 presents PEEM images of fibrinogen molecules adsorbed onto an *n*-type silicon substrate. Figure 4(a) was obtained at a field of view of 1.5 μm, with the FEL emission tuned to 238.5 nm (5.2 eV) and Fig. 4(b) is an enlarged section of the image, which displays the trinodular structure of a single fibrinogen molecule. The inset in Fig. 4(b) shows a schematic of fibrinogen at the appropriate magnification. This is the specific image that was used to obtain the photoionization threshold data. To justify the presence of single fibrinogen molecules, we imaged the sample with atomic force microscopy prior to the PEEM measurements. Single fibrinogen molecules, with a well resolved trinodular structure, were evident over the silicon surfaces. The images are not shown here.

B. Modeling of the wavelength-dependent PEEM emission

In the study of photoelectric phenomena in solids, Fowler[15] reported a method in 1931 which described the photoelectric current of the clean metals near the threshold, taking the temperature effect into account. The photoemission data of silver, gold, tantalum, tin, and potassium were analyzed based on this model, and the measured values of photocurrent as a function of temperature and incident light displayed excellent agreement with the theoretical fit. In this treatment, the photocurrent per unit incident light intensity is described by

$$\frac{I(\chi_0 - h\nu)^{1/2}}{T^2} = Af(\mu) = Af\left(\frac{h\nu - \chi}{kT}\right), \tag{2}$$

where A is a scaling constant independent of ν and T. In the above equation, $f(u)$ is a term by term integration of the number of available electrons in a certain energy range described by Fowler and is given by

$$f(u) = e^u - (e^{2u}/4) + (e^{3u}/9) - \cdots \quad (u \leqslant 0),$$

$$f(u) = (\pi^2/6) + (u^2/2) - [e^{-u} - (e^{-2u}/4) + (e^{-3u}/9) - \cdots] \quad (u \geqslant 0). \tag{3}$$

The values of the scaling constant A and the photothreshold χ can be determined by a curve fitting software using an iterative Levenberg-Marquardt algorithm that minimized the chi-square value. The temperature of the sample surface in PEEM measurements was measured with a thermocouple attached to the sample holder, and the temperature maintains a constant value of 298 K. Therefore, this value was utilized in the fitting calculations.

A simplified form of the Fowler equation has been used as follows to calculate the photoionization threshold potential of metals when temperature is not a significant factor:

$$I^{1/2} = A(h\upsilon - E_T). \tag{4}$$

This equation is referred to as the square-root law in the following discussions. In the above expression, the photoionization threshold potential E_T is obtained by determining the value of υ, where $I^{1/2} \rightarrow 0$. This procedure ignores any contributions to the photocurrent due to the thermal distribution of energies in the sample.

For Kane's theory of photoelectric emission from semiconductors,[16] it was noted that the direct and indirect excitation processes display a photoionization yield proportional to $E-E_T$ and $(E-E_T)^{5/2}$, respectively. Both processes appear to have been identified experimentally by Gobeli and Allen on the atomically clean (111) silicon surfaces.[17] Kochi *et al.*[18] observed that Kane's power laws mainly depend on the shape of the upper edge of the valence band and should not be applied to organic crystals with typically narrow valence bands. A semiempirical power law for the yield of organic crystals near the threshold was proposed as follows:

$$Y \propto (h\upsilon - E_{\text{th}})^m \left(\frac{5}{2} \leqslant m \leqslant 3\right), \tag{5}$$

where the quantum yield Y is designated by Y=number of electrons emitted/number of incident quanta. The assumption that all the incident quanta are adsorbed was made.[18] This equation is referred to as the cube-root law in the following discussions. The above expression was determined to be in good agreement with the experimental results of the photoelectric yield near the threshold for anthracene single crystal.[18]

Figure 5 shows the analysis of the photoionization threshold potential of single fibrinogen molecules adsorbed onto n-type silicon substrates. Three fitting models were employed to obtain the threshold value. The experimental data (dots) are fitted with (a) temperature dependent Fowler law, (b) square-root law, and (c) cube-root law, which provide thresholds of 4.9, 5.0, and 5.0 eV, respectively.

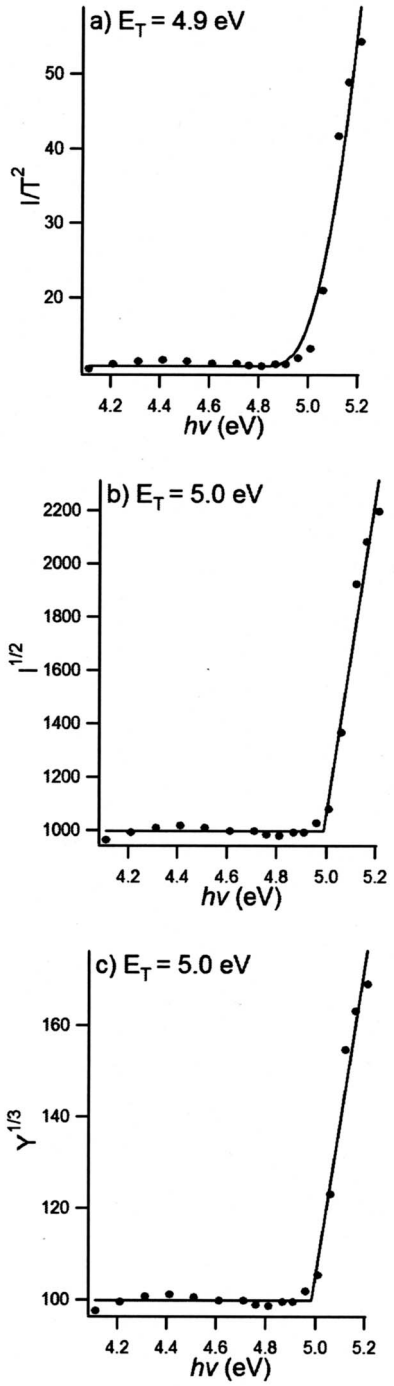

FIG. 5. Photoionization potential threshold data shown in (a)–(c) are determined from a single fibrinogen molecule adsorbed onto n-type silicon surfaces using PEEM. The experimental data (dots) fit with the temperature dependent Fowler equation is shown in (a). (b) and (c) show the data fit with the square-root law and the cube-root law, respectively.

IV. DISCUSSION

The system of biological molecules adsorbed onto a substrate is complex to quantitatively determine the threshold of photoionization energies, especially at the single molecule level. To the best of our knowledge, no theoretical models have been proposed for this system yet. The photoemission process of these samples is different from that of metals or inorganic semiconductors that exhibit extensive bond delocalization in the solid state. This is because in metals and semiconductors, the photoemission results in a rearrangement of conduction or valence band electrons compared to

the relatively localized electron states at the photothreshold in biological molecules. The models of organic crystals and organic films need to be questioned when used in a single biological molecule system that posseses no intermolecular interactions. Wilson *et al.*[19] obtained the threshold ionization energies for biological nanoparticles by extrapolating to zero the kinetic energy of photoelectrons versus the incident photon energy. The threshold value was checked using the square-root Fowler law by extrapolating to zero the electron yield, which resulted in exactly the same value. Our results show that the photoionization threshold of a single fibrinogen obtained from the three fitting approaches exhibited the same values within the error of these measurements. We utilized the spontaneous emission mode of the Duke UV-FEL in the spectral range of 229.5–302.4 nm (5.4–4.1 eV), with an energy full width at half-maximum of ~0.1 eV. By accounting for other uncertainties of data acquisition, including measurements of laser power and image drifting artifacts, the total uncertainty of the photoionization threshold measurements from PEEM is ~0.2 eV. The threshold difference from fitting calculations with temperature dependent Fowler law, square-root law, and cube-root law is less than the uncertainty of the measurements.

There is usually sufficient conductivity for the biological specimens to avoid charging, and charging was not observed in these measurements. The intensity did not change over time although no fixing or coating of the molecules was done in the sample preparation. We suggest that the electrons emitted from fibrinogen molecules are replaced from the silicon substrates.

V. CONCLUSIONS

By using the imaging capabilities of PEEM in conjunction with the tunability of the Duke UV-FEL, the spatially resolved photothreshold of a biological sample was measured and a procedure for these measurements at a single molecule level is established. The data acquisition and correction is reviewed and applied to samples of human plasma fibrinogen adsorbed onto *n*-type silicon substrates. Three theoretical models, including that for metals based on temperature dependent Fowler law, that for semiconductors based on Kane's power law, and that for organic crystals based on a cube-root law, were used to fit the experimental data of the photocurrent versus incident photon energy. The results exhibited thresholds of 4.9, 5.0, and 5.0 eV, respectively, using the three fitting models. The difference is less than the uncertainty of the measurements of ±0.2 eV. We conclude that the temperature dependent Fowler law, square-root law, and cube-root law do not result in significant deviation and can be equally used to analyze the photoionization threshold potential of biological samples at the single molecule level.

ACKNOWLEDGMENTS

This research was carried out as part of the Advanced Carbon Nanotechnologies Program and the AFOSR through the MFEL program at Duke University. The authors acknowledge the Duke University Free Electron Laser Laboratory, where all of the photoelectron emission microscopy experiments were performed. Discussions with Jingyi Li regarding the FEL are gratefully acknowledged.

[1] R. W. Colman, J. Hirsh, V. J. Marder, A. W. Clowes, and J. George, *Hemostasis and Thrombosis: Basic Principles and Clinical Practice* (Lippincott, Philadelphia, 1994).
[2] C. N. Cottonaro, H. V. Roohk, G. Shimizu, and D. R. Sperling, Trans. Am. Soc. Artif. Intern. Organs **27**, 391 (1981).
[3] P. D. Hoeprich and R. F. Doolittle, Biochemistry **22**, 9 (1983).
[4] B. Gradlund, B. Hessel, G. Marguerie, G. Murano, and B. Blomback, Eur. J. Biochem. **77**, 3 (1977).
[5] Z. Yang, J. M. Kollman, L. Pandi, and R. F. Doolittle, Biochemistry **40**, 42 (2001).
[6] C. E. Hall and H. S. Slayter, J. Biophys. Biochem. Cytol. **5**, 1 (1959).
[7] T. A. Horbett, Cardiovasc. Pathol. **2**, 3 (1993).
[8] B. D. Ratner, A. S. Hoffman, F. J. Schoen, and J. E. Lemons, *Biomaterials Science: An Introduction to Materials in Medicine* (Academic, San Diego, 1996).
[9] G. B. Birrell, D. L. Habliston, and O. H. Griffith, Biophys. J. **67**, 5 (1994).
[10] O. H. Griffith and G. F. Rempfer, Annu. Rev. Biophys. Bioeng. **14**, 113 (1985).
[11] D. L. Habliston, K. K. Hedber, G. B. Birrell, G. F. Rempfer, and O. H. Griffith, Biophys. J. **69**, 4 (1995).
[12] G. B. Birrell, K. K. Hedberg, D. L. Habliston, and O. H. Griffith, Ultramicroscopy **36**, 1 (1991).
[13] A. Samokhvalov, L. Hong, Y. Liu, J. Garguilo, R. J. Nemanich, G. S. Edwards, and J. D. Simon, Photochem. Photobiol. **81**, 1 (2005).
[14] H. Ade *et al.*, Surf. Rev. Lett. **5**, 6 (1998).
[15] R. H. Fowler, Phys. Rev. **38**, 45 (1931).
[16] E. O. Kane, Phys. Rev. **127**, 131 (1962).
[17] G. W. Gobeli and F. G. Allen, Phys. Rev. **127**, 141 (1962).
[18] M. Kochi, Y. Haraka, T. Hirooka, and H. Inokuchi, Bull. Chem. Soc. Jpn. **43**, 9 (1970).
[19] K. R. Wilson, D. S. Peterka, M. Jimenez-Cruz, S. R. Leone, and M. Ahmed, Phys. Chem. Chem. Phys. **8**, 16 (2006).